Journal of the Textile Institute
Publication details, including instructions for authors and subscription information:
http://www.informaworld.com/smpp/title~content=t778164490

Compression behavior evaluation of single down fiber and down fiber assemblies

Jing Gao [ab]; Ning Pan [c];Weidong Yu [a]
[a] College of Textiles, Donghua University, Shanghai, People's Republic of China [b] Key Laboratory of Textile Science & Technology, Ministry of Education, People's Republic of China [c] Biological and Agricultural Engineering Department, University of California at Davis, California, USA

First published on: 08 January 2010

To cite this Article Gao, Jing , Pan, Ning andYu, Weidong(2010) 'Compression behavior evaluation of single down fiber and down fiber assemblies', Journal of the Textile Institute, 101: 3, 253 — 260, First published on: 08 January 2010 (iFirst)
To link to this Article: DOI: 10.1080/00405000802377342
URL: http://dx.doi.org/10.1080/00405000802377342

The Journal of The Textile Institute
Vol. 101, No. 3, March 2010, 253–260

Compression behavior evaluation of single down fiber and down fiber assemblies

Jing Gao[a,b]*, Ning Pan[c] and Weidong Yu[a]

[a] *College of Textiles, Donghua University, Shanghai, People's Republic of China;* [b] *Key Laboratory of Textile Science & Technology, Ministry of Education, People's Republic of China;* [c] *Biological and Agricultural Engineering Department, University of California at Davis, California, USA*

(*Received 3 May 2008; final version received 29 July 2008*)

Down fibers have superior thermal insulating properties as natural nonwoven and filler materials. Physical properties include single-fiber bending, down assembly bulkiness, compressibility and recoverability, which all affect down fibers' thermal insulation greatly. Research on the physical properties of down fibers has been very limited. In this paper, the physical property tests and analyses on both single down fibers and down fiber assemblies were carried out seriatim. The fiber bending properties were tested by an axial-buckling method, and the assembly compressibility and recoverability were tested by fiber assembly conductivity analyzer. The behavior mechanisms were explained by fiber structure and arrangement factors. Synchronously, the physical properties of down are evaluated and compared with other kinds of keratin fibers and wool.

Keywords: down fiber; bending property; fiber assembly; compressibility; recoverability

Introduction

Down fibers are used widely in insulated textile products, especially in insulated winter outerwear because of their superior thermal-insulating properties and soft touch. The physical properties of down fiber and down fiber assembly i.e. the bending rigidity and bending modulus are the key determinants. Down fiber assemblies have high bulkiness to hold plenty of air and great resilience after compression to retain the entrapped air and thus provide thermal insulation. The fibers' soft handle mainly results from the lower bending modulus and flexural rigidity of down fibers and the great compressibility of down assemblies.

In spite of the long history and extensive applications of the down hair, documented knowledge on down's physical properties' research is scarce. We have only been able to identify a couple of papers specifically, albeit briefly and qualitatively, devoted to the analyses of the structure and properties of down fibers and down assembly (Gao, Pan, & Yu, 2007; Skelton, Dent, & Donovan, 1985; Wu & Song, 1990). In addition, there have been a few studies on the bending stress–strain properties of single fibers (Carlene, 1947; Peirce, 1930), wool, alpaca fiber, and silk fiber in particular (Liu, 2004; Yu & Liu, 2006). There have also been a few papers are on the properties of poultry feathers (Schmidt & Line, 1996; Whitt, Hess, Bilgili, & Broughton, 1997), specifically chicken (Ye & Broughton, 2002), and turkey feathers (George, Bockarie, McBride, Hoppy, & Scutti, 2003). In this paper the integrative physical properties of down fibers and down fiber assembly are studied and evaluated based on the fiber compression bending analyzer (Liu, 2004) and the fiber assembly conductivity analyzer (Yu & Liu, 2005).

Experimental procedures

Single down fiber bending

Test principle

Axial bending properties of single fiber were tested on the fiber compression bending analyzer (Liu, 2004; Yu & Liu, 2006), whose configuration is shown in Figure 1. Based on the *critical load rule*, proposed by Euler, one end of the fiber was fixed, and the other was pinned. The fiber was axially compressed between the mechanical stage and the loading piece, to determine the relationship of the critical force and the displacement. Figure 2 expressed the axial compression bending model (Liu, 2004).

The theoretical mode (Liu, 2004) of axial bending of the fiber is given by

$$P_{cr} = (kL)^2 \frac{EI}{L^2} = \frac{20.19EI}{L^2}, \qquad (1)$$

where P_{cr} is the critical loads (cN); k is the exchange coefficient; L is the effective length of the fiber (cm); E is

---

*Corresponding author. Email: gao2001jing@dhu.edu.cn

ISSN 0040-5000 print / ISSN 1754-2340 online

DOI: 10.1080/00405000802377342
http://www.informaworld.com

Figure 1. Fiber compression bending analyzer.

the elastic modulus; I is the fracture inertial moment; and EI is the bending rigidity of fiber (cN·cm^2). Thereby, the bending rigidity is given by

$$EI = \frac{P_{cr}L^2}{20.19}. \quad (2)$$

Considering the effects of the fiber cross-section on the fracture inertial moment I, the section shape coefficient η_f to Equation (1) is introduced here. With the circular section radius r, the minimum inertial moment I_0 is

$$I_0 = \frac{\pi r^4}{4}. \quad (3)$$

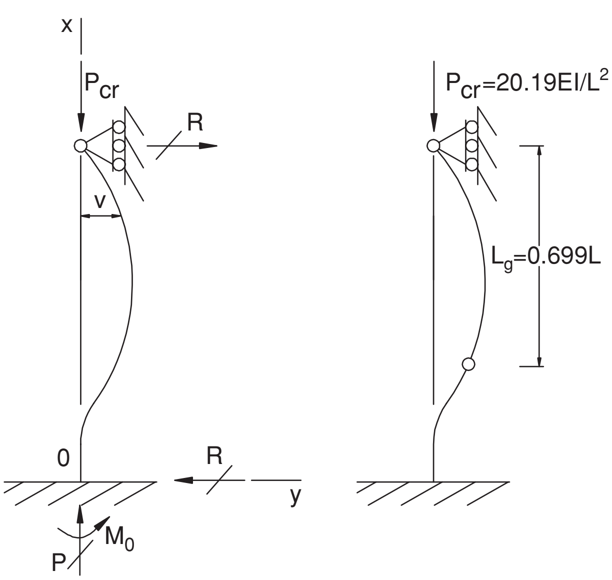

Figure 2. Model of axial compression bending.

So the critical loads would be given by

$$P_{cr} = \frac{20.19 E_B \eta_f I_0}{L^2} = \frac{20.19 \pi r^4 E_B \eta_f}{4L^2} = (0.99 E_B \eta_f)\frac{D^4}{L^2}. \quad (4)$$

Because the cross-section of down branch fibers is ellipse (Gao et al., 2007), and the coefficient η_f is approximate 0.736, the mean bending modulus of down branch is

$$E_B = \frac{1.01 \times 10^{-8} P_{cr} L^2}{\eta_f D^4} = \frac{1.01 \times 10^{-8} P_{cr} L^2}{0.736 D^4} = \frac{1.37 \times 10^{-8} P_{cr} L^2}{D^4} \quad (5)$$

in which D is the mean reduced diameter of down branch, and the unit of P_{cr} is dyne, D is mm, L is mm, and E_B is Gpa.

According to the theoretical model of fiber axial bending, the load force could be measured and the bending modulus of single fiber would thus be calculated at the critical load just described.

Preparation of samples

The fiber samples were conditioned for more than 24 h under the standard temperature of 20°C and relative humidity of 65%. The bottom of the fiber was clamped by the adhesive plastic embedded in a metal groove to simulate the fixed end, and the top end of the fiber was grounded into a platen covered with sandpaper, avoiding fiber tip slippage to simulate the pinned end. The protruded length of the fiber was determined by the fineness of the fiber (Figure 3), which means that the fiber slenderness (length/fineness) should be appropriate. The fiber was neither too short, being compressed directly to yield, nor too long, avoiding the very small critical force load.

Here we believe that the down branch is the primary bearing part of down, and the bending of the down branch is the leading behavior. The effects of the fibrils diverging from the down branch are expected to be minimal (see Figure 3a). Then, the axial bending strength of the down branch fiber was measured using the fiber compression bending analyzer, in which the down branch was compressed by dropping the top surface, and the compressive force was directly tested by a load cell. The axial displacement was calculated by the loading time and the crosshead speed. The crosshead speed was 0.1 mm/s for the 2-mm long down branch.

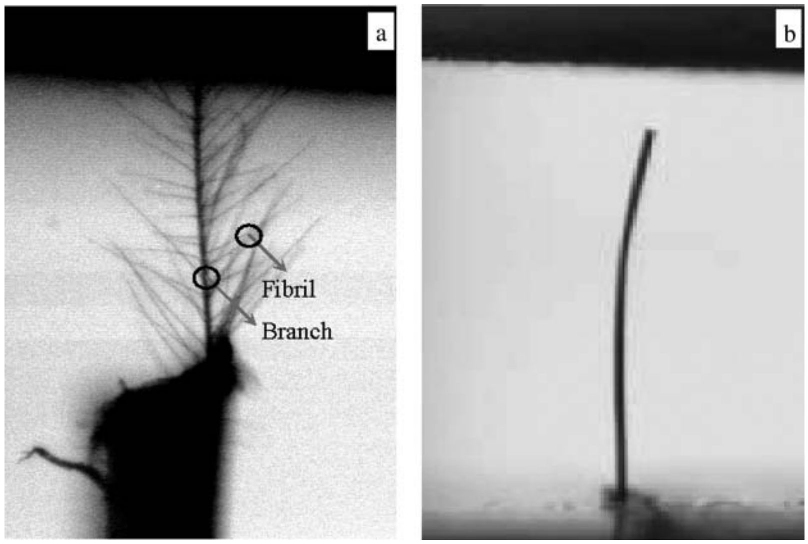

Figure 3. Sample preparation (a) down and (b) wool.

Compression recovery of down fiber assemblies

The compression-recovery tests were carried out based on the fiber assembly conductivity analyzer (Yu & Liu, 2005), as shown in Figure 4, developed by Tension Member Technology (TMT) lab in Donghua University. This system realizes the dynamic and continuous measurements of compression and reversion course of loose fiber assembly. As the volume fraction of assembly continually changed, the curves with displacement and pressure were recorded synchronously.

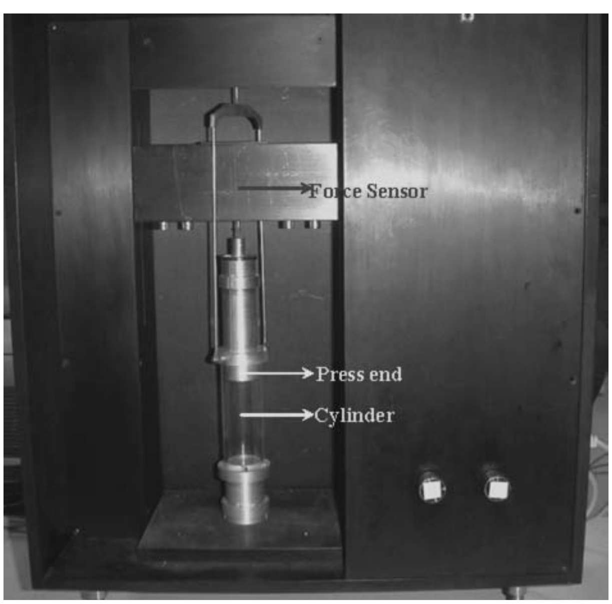

Figure 4. Fiber assembly conductivity analyzer.

After the loose fiber assembly samples were conditioned for more than 24 hr under standard atmosphere, the quantitative loose samples were put into the cylinder signed scale shown in the Figure 4. As *press end* moved down at 10 cm/min, the fiber assembly was compressed; at the same time it returned equality pressure to the press end, which was recorded by the *force sensor* fixed at the press end. Thereby the compression curves were synchronously recorded on the computer with displacement and pressure (Figure 5). The pressure increased continuously until the press end arrived at the downmost position. Here, when the press end moved up, the fiber assembly bounced in good time. Then the pressure on the force sensor decreased gradually, and at the same time the resilience curves were recorded accordingly (Figure 5). The *compression rate* (C), *recovery rate* (R), and *volume fraction* (V_f) are respectively given by

$$C = \frac{H_1}{H_0} \times 100\%, \;\; R = \frac{H_2}{H} \times 100\%, \;\; \text{and } V_f = \frac{v_f}{v},$$

in which H_0 is the initial height of fiber assembly in the cylinder; H_1 is the distance of fiber assembly moving down under pressure; H is the height of fiber assembly down most; H_2 is the moving distance of the fiber assembly from the downmost place to the rest place after the pressure is lost; v_f is the fiber volume; and v is the assembly volume.

Results and discussion

Bending modulus of single down fiber

According to Equation (4), the *critical force* P_{cr} is proportional to D^4/L^2, and the corresponding experimental data are shown in Figure 6. The regressive equation for down

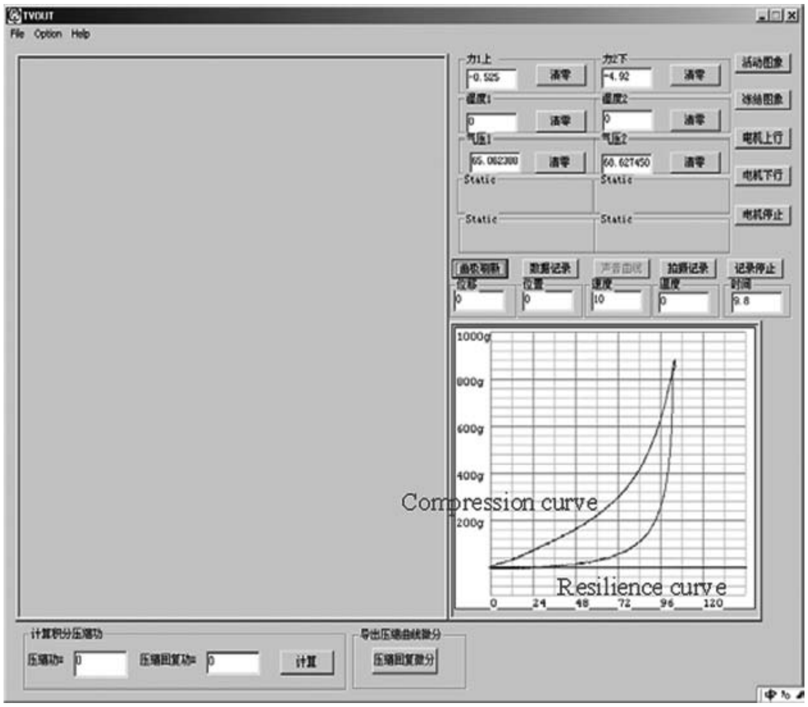

Figure 5. Compression-recovery test on computer.

fiber is $P_{cr} = (4.826 \times 10^7)D^4/L^2$, and the correlation coefficient R^2 is 0.8018. The down had lower R^2 than the wool, due to the somewhat big change of the fineness along the down branch axis.

The bending properties of the single fiber could be quantified by calculating the equivalent bending modulus and the flexural rigidity. The equivalent bending modulus and the flexural rigidity could be calculated by measuring the critical force and the fiber length and diameter. Fiber structure determined the critical force. The correlative parameters of the down branch and the wool are given in Table 1.

The measured data show that the equivalent bending modulus of the down branch was much lower than that of the wool. The rigidity of the down was 1/10 th as low as wool. This revealed that the down branch was much easier to compress under less force than the wool. Thereby, the down and the down assembly were provided with soft handle.

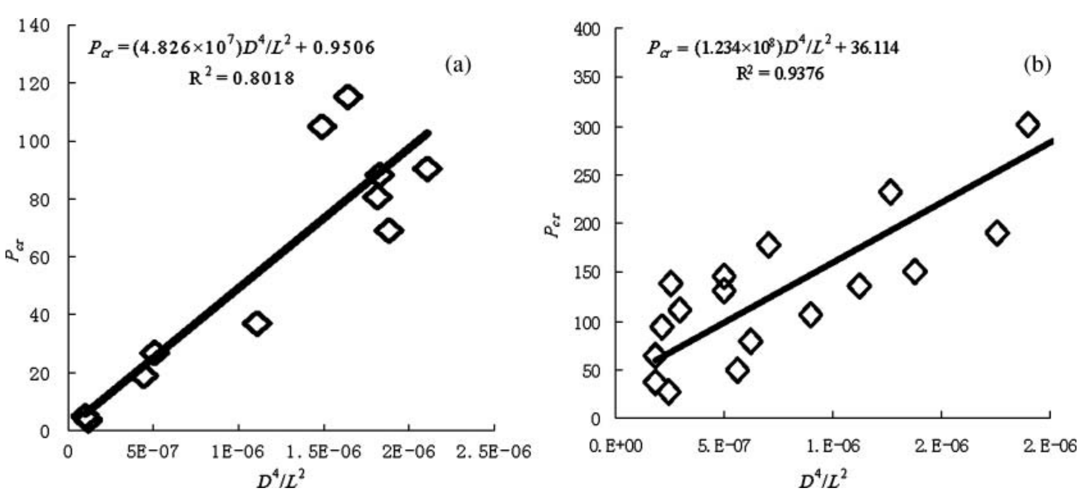

Figure 6. The relationship of critical force with D^4/L^2 (a) down and (b) wool.

Table 1. Bending properties of down branch and wool.

Samples	L (mm)	D (μm)	P_{cr} (dyn)	η_f	EI (10^6 cN · cm^2)	E_B (Gpa)
Down branch	0.563	24.16	63.59	0.74	9.98	0.81
Wool	0.959	36.44	303.5	0.88	138	1.82

Bending-recovery curves of single down fiber

The typical load-displacement plots recording fiber bending and recovery are shown in Figure 7. The critical force represents the maximal carrying capacity of the single fiber. When the stress on outer fibrils exceeded the proportional limit, the fiber didn't follow Hooke's law any longer. The slope of the curve didn't change until the force arrived at the proportional limit. Then the load reached a maximum, that is, the critical force. After that point, the increasing stress resulted in fiber yielding, and the curve turned down.

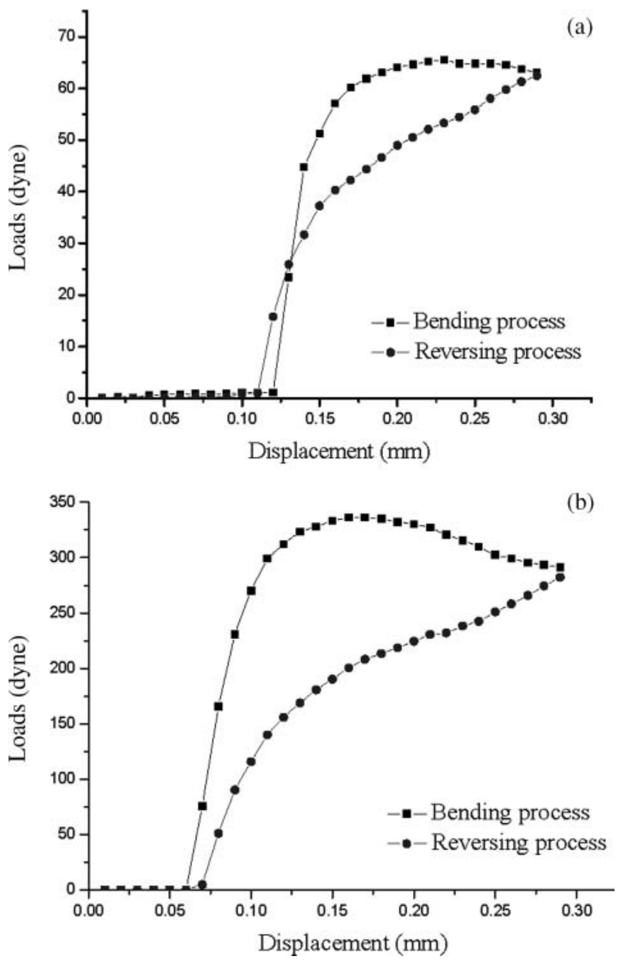

Figure 7. Bending-recovery curves of single fiber (a) down and (b) wool.

The load-displacement curve was determined by the fiber's bending properties and slenderness.

The recovery curve after unloading did not follow the bending curve under loading, and a relatively big bending hysteresis loop was produced. The possible explanation for this behavior is the internal friction and slippage between the fibrils and the molecular chains. In addition, the hysteresis loss would partially attribute to the compression hysteresis of the whole assembly. Compared with wool, down had less hysteresis loss despite its lower bending modulus.

Generally, hysteresis loss meant bending breakage, which could be characterized by bending-work restitution coefficient (W). If the area composed by bending curve and X-axis is S and by recovery curve and X-axis is S', then S is called bending work, and $W = S'/S$. From Figure 7, it can be seen that the bending work S of the wool fiber is much larger than that of the down, which proves that resistance to bending of the wool is stronger than that of the down. However, the bending-work restitution coefficient of down was larger than that of wool in spite of the lower bending work of down. It revealed the internal delamination and slippage between fibrils of down were not so evident as those of wool during the whole bending course, due to the more compact crystal structure in down (Gao, et al., 2007) than in wool with medulla lumen.

Compressibility of down fiber assembly

The *pressure–*V_f curves of down fiber assemblies with various *initial volume fractions* (V_0) are shown in Figure 8. It can be seen that the *volume fraction* (V_f) increased much more obviously as the pressure enhanced when V_0 was less. Two factors worked on it: one was the less bending resistance provided by the less numbers of fibers, and the other was the larger void volume among fibers. Contrarily, when

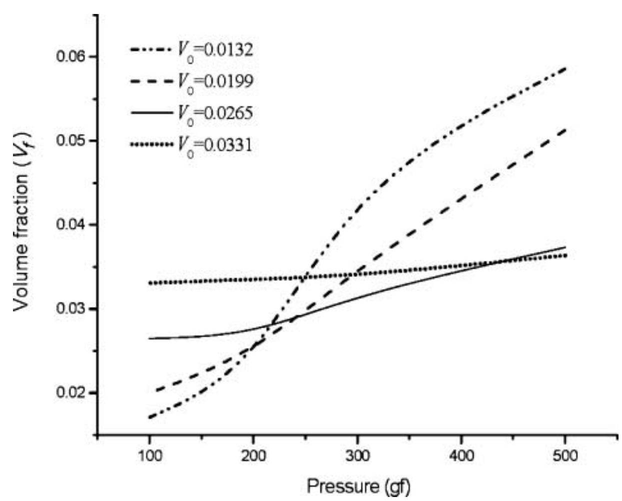

Figure 8. *Pressure–*V_f curves of down fiber assemblies with various initial volume fraction (V_0).

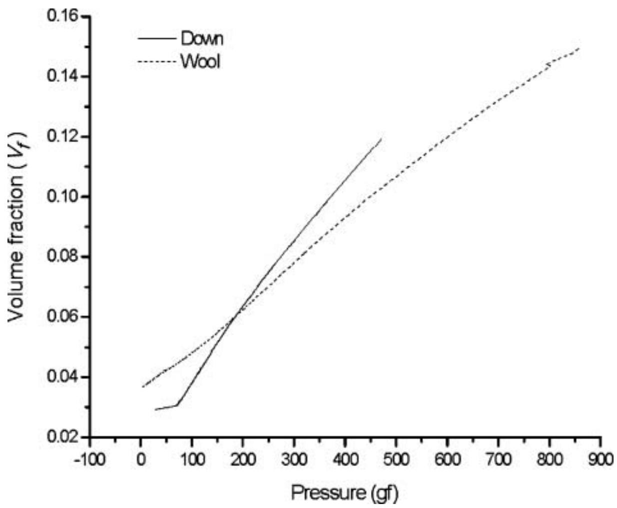

Figure 9. *Pressure–V_f* curves of down and wool fiber assemblies with $V_0 = 0.0315$.

V_0 became larger, the flex resistance provided by the fibers was stronger, and the fractional void providing deformation decreased for the more compact contact among fibers. So the V_f increased less, as the pressure enhanced. Considered the curve of $V_0 = 0.0132$ as explanation; when V_0 was less, the curve had typical compression characters. Under low pressure, less deformation of the assembly mainly resulted from the bending of fibers on the up side of the assembly. As the pressure increased, more fibers joined to bend, and much slippage among fibers took place. The void in assembly decreased quickly, and the assembly finished the main deformation. As the pressure on assembly enhanced unceasingly, only a little porousness provided the deformation, and a few fibers slippage processed. The deformation volume of assembly reduced accordingly.

The *pressure–V_f* curves of down and wool fiber assemblies with $V_0 = 0.0315$ are shown in Figure 9. From the figure we could see that, as the pressure enhanced gradually, the volume of down assembly decreased more obviously than that of wool. It proves that down assembly has a better compressibility than wool. The interpretive reasons are the great bulkiness of down assembly, providing a mass of pores for assembly deformation. At the same time, the lower bending rigidity of single down fiber, bringing down assembly less compression resistance, was the other important factor. The bulkiness of down and wool fiber assemblies are shown in Table 2.

Table 2. Bulkiness and density of down and wool fiber assemblies.

	V_o (cm^3)	*m* (g)	Bulkiness (cm^3/g)	Density (g/cm^3)
Down assembly	500	1.43	349.65	0.00286
Wool assembly	500	5.06	98.81	0.01012

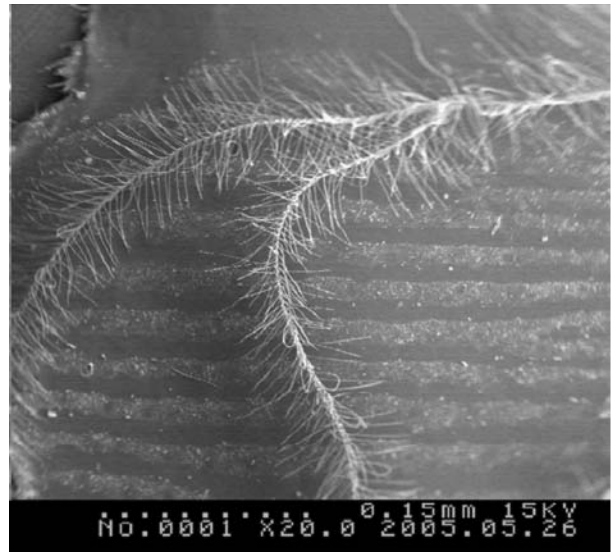

Figure 10. Down fibrils on down branches.

As seen in Figure 9, a slow change course of V_f during primal pressure of 0∼70 gf was also discovered. The possible explanation for this behavior is the down special bifurcate structures on both the down branch (Figure 10) and the down fibrils (Figure 11). As the pressure was slight, the plentiful fibrils on down branches and the triangle nodes and crotches on down fibrils would momently sustain the down branch against bending.

Recovery ability of down fiber assembly

The compression-recovery curves of down and wool fiber assemblies are shown in Figure 12. During the compression

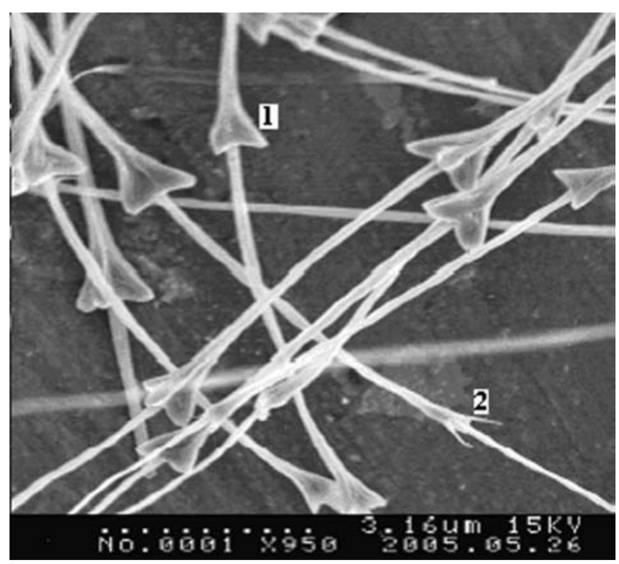

Figure 11. Triangle nodes (1) and crotches (2) on down fibrils.

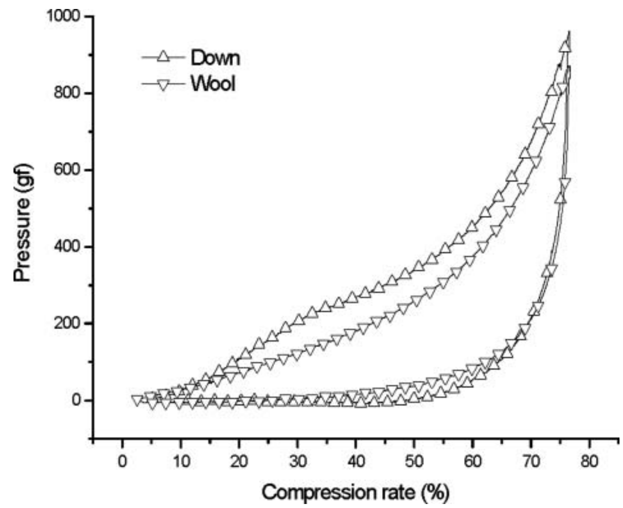

Figure 12. Compression-recovery curves of down and wool fiber assemblies.

and recovery process, compression hysteresis loops were produced, due to the fiber slippage and single-fiber bending hysteresis. Compared with wool, down fiber assembly had more compression hysteresis loss. This proved that down fiber assembly had lower compression-recovery ability than wool, even if single down fiber had higher bending recovery ability than wool. Here the functions of the special bifurcate structures on both down branches and down fibrils have to be mentioned. They intervened with and embedded each other when the assembly was compressed, and with the pressure lost, this insetting frame would prevent each other from moving greatly. This resulted in the down fiber assemblies facing difficulty in bouncing, so the recovery curve produced a larger hysteresis loop (Figure 12). In order to resolve the large hysteresis, the appropriate agitation

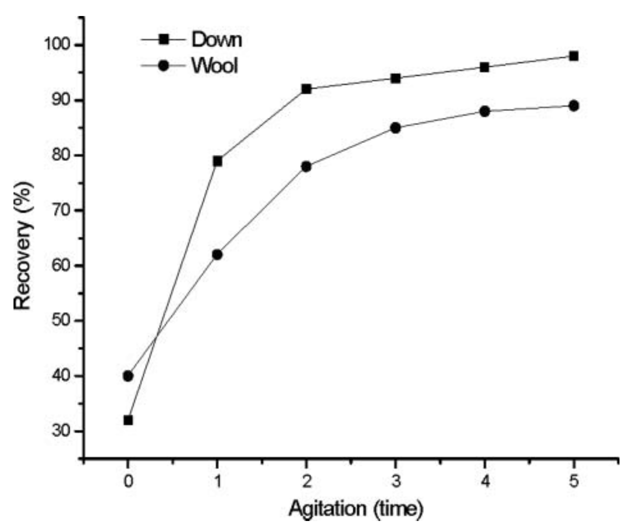

Figure 13. Recovery of down and wool fiber assemblies under agitation.

relieved the intercrossing effectively. Figure 13 shows the recovery of down and wool fiber assemblies under agitation. Because the bifurcate structures provided specifically located, but not permanent, contact point of fiber with fiber and generated a preferred intercontact distance, the agitation could availably unlock the nodes and crotches and make the contacts among fibers separate on the instant. So the fiber assembly could revert to the fluey state quickly under agitation.

Conclusions

Physicomechanics of fiber itself influenced assembly compression and recovery, so the bending properties of single down branch were quantitatively analyzed at first in this paper. The data show that the equivalent bending modulus of down fiber is much lower than wool, and the rigidity is 1/10th as low as that of wool. There is a hysteresis loop during bending and recovery courses of single fiber, the possible explanation for which is the internal friction and slippage between the fibrils and the molecular chains. Down has less hysteresis loss than wool, because of which it is considered that down has better bending-recovery ability than wool. We think that it might be owed to the more compact crystal structure of down.

Down fiber assembly has the better compressibility than wool. The morphological structure and physical properties of single down fiber are considered to greatly contribute to that. The large numbers of bifurcate structures on both the down branch and down fibrils could occupy abundant space and make down fiber assembly greatly bulky. That provides enough porousness for assembly deformation. In addition, the lower bending rigidity of single down fiber is the other factor to make assembly compress easily. When the pressure on assembly is slight, the plentiful fibrils on down branches and the triangle nodes and crotches on down fibrils extend provisional support function to the down branches. So the V_f of the assembly has a slow change phase at the primal pressure of 0–70 gf. Contrarily, when the pressure vanishes, the bifurcate structures prevent assembly recovery again. So the down fiber assembly exhibits poor compression-recovery ability. The appropriate agitation is an effective approach to unlock the intercrossing among the fibrils or the nodes or the crotches and make the contacts among fibers separate on the instant.

In addition, the lower bending rigidity of single down fiber and the better compressibility of down fiber assembly mainly contribute to the soft handle of down and down assembly.

Acknowledgement

This work was supported by Grant No. 50806011 from the National Natural Science Foundation of China.

References

Carlene, P.W.J. (1947). The measurement of the bending modulus of monofils. *Journal of Textile Institute, 38*, T38–T42.

Gao, J., Yu, W.D., & Pan, N. (2007). Structures and properties of the goose down as a material for thermal insulation. *Textile Research Journal, 77*, 617–626.

George, B.R., Bockarie, A., McBride, H., & Hoppy, D., Scutti, A. (2003). Utilization of turkey feather fibers in nonwoven erosion control fabrics. *International Nonwovens Journal, 4*, 45–52.

Liu, Y.Q. (2004). Master's dissertation. Donghua University, People's Republic of China.

Peirce, F.T. (1930). The 'handle' of cloth as a measurable quantity. *Journal of Textile Institute, 21*, 377–416.

Schmidt, W.F., & Line, M.J. (1996). Physical and chemical structure of poultry feather fiber fractions in fiber process development. In Proceedings of the TAPPI Nonwovens Conference, Charlotte, North Carolina.

Simitses, G. (1976). *Introduction to the elastic stability of structures*. Englewood Cliffs: Prentice Hall.

Skelton, J., Dent, R., & Donovan, J.G. (1985). Proceedings of the 7th International Wool Textile Research Conference: Vol. 3 (pp. 237–288).

Whitt, J.S., Hess, J.B., Bilgili, S.F., & Broughton, R.M. (1997). *Poultry Science, 76*, 11.

Wu, A.C., & Song, X.C. (1990). Structure and properties of feather and down. *Journal of China Textile University, 2*, 94–98.

Ye, W., & Broughton, R.M. (2002). Chicken feather as a fiber source for nonwoven insulation. *International Nonwovens Journal, 3*, 113–121.

Yu, W.D., & Liu, Q. (2005). Patent. 2005, 10024967.4.

Yu, W.D., & Liu, Y.Q. (2006). Softness evaluation of keratin fibers based on single-fiber bending test. *Journal of Applied Polymer Science, 101*, 701–707.